REAL-TIME TRAFFICKING AND ASSEMBLY OF RIBOSOMAL SUBUNITS

A Senior Honors Thesis

by

JASON WANG

Submitted to the Office of Honors Programs
& Academic Scholarships
Texas A&M University
in partial fulfillment of the requirements of the

UNIVERSITY UNDERGRADUATE
RESEARCH FELLOWS

April 2004

Majors: Genetics and Biochemistry

REAL-TIME TRAFFICKING AND ASSEMBLY OF RIBOSOMAL SUBUNITS

A Senior Honors Thesis

by

JASON WANG

Submitted to the Office of Honors Programs
& Academic Scholarships
Texas A&M University
in partial fulfillment of the requirements of the

UNIVERSITY UNDERGRADUATE
RESEARCH FELLOWS
Approved as to style and content by:

Siegfried M. Musser
(Fellows Advisor)

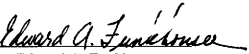

Edward A. Funkhouser
(Executive Director)

April 2004

Majors: Genetics and Biochemistry

ABSTRACT

Real-Time Trafficking and Assembly

of Ribosomal Subunits. (April 2004)

Jason Wang
Department of Biochemistry and Genetics
Texas A&M University

Fellows Advisor: Dr. Siegfried M. Musser
Department of Medical Biochemistry and Genetics

Nuclear pore complexes (NPCs) facilitate the bidirectional transport of a myriad of molecules, ranging in size from an ion to assembled ribosomal subunits, across the two lipid bilayers that constitute the nuclear envelope (NE). Research over the past decade has imparted much insight into how NPCs control the selective passage of large macromolecules while maintaining their compartmentalization properties. Schemes for soluble cofactor-mediated active transport have been developed through phenotypic mutational analyses and *in vitro* experiments. Continuing the effort for a more comprehensive characterization of NPC function, we have developed a method for the *in vivo* analysis of nucleocytoplasmic transport utilizing fluorescently labeled, recombinant human ribosomal protein L23a (rpL23a-His). Cytoplasmic microinjections into live HeLa cells indicated rapid nuclear import and subsequent export of rpL23a-His. These results are expected to lead to real-time *in vivo* single-molecule observation of ribosomal subunit trafficking and assembly.

ACKNOWLEDGMENTS

I would like to thank Dr. Siegfried M. Musser for his amazing guidance, remarkable patience, and immeasurable willingness to educate. I would also like to thank Dr. Weidong Yang for his supportive advice on putting together this thesis and Dr. Umesh K. Bageshwar for his help with the N-terminal sequencing interpretation and analysis.

TABLE OF CONTENTS

LIST OF FIGURES

LIST OF ABBREVIATIONS

NPC – nuclear pore complex

NE – nuclear envelope

rpL23a – human ribosomal protein L23a

6xHis – six consecutive histidines

rpL23a-His – recombinant human ribosomal protein L23a with a 6xHis-tag, a cysteine, and a glutamic acid

RanGAP – RanGTPase activating protein

NTF2 – nuclear transport factor 2

NLS – nuclear localization signal

PVP – polyvinylpyrrolidone

PVDF – polyvinylidene fluoride

Ac – acetate

DIC – differential interference contrast

MW – molecular weight

SDS-PAGE – sodium dodecyl sulphate polyacrylamide gel electrophoresis

NLS-2xGFP – two tandem green fluorescent proteins with an NLS leader peptide

ER – endoplasmic reticulum

INTRODUCTION

The double membrane nuclear envelope (NE) of eukaryotic cells isolates the genetic material in the nucleoplasm. Consequently, gene regulatory signals originating cytoplasmically or extracellularly must cross this permeability barrier to access their downstream targets. Newly synthesized RNAs and recently assembled ribosomal subunits must also transit across the NE to reach the cytoplasm. The gatekeepers that regulate this molecular traffic between nucleus and cytosol are the macromolecular assemblies known as nuclear pore complexes (NPCs). NPCs allow the passive diffusion of ions and molecules up to 9 nm (20-40 kDa) (1), and yet are capable of mediating the signal-dependent transport of macromolecules as large as 39 nm in diameter (2). For small, diffusable proteins carrying nuclear localization signals (NLS), active transport is often favored over passive diffusion by transport receptor binding to the NLS (3, 4).

Active transport of macromolecules through the NPC is an orchestrated process that requires soluble transport cofactors which recognize cargo and assist their passage through the aqueous central channel of NPCs. Importin β-like transport receptors comprise a superfamily of transport cofactors which mediate the bidirectional transport of the majority of proteins and RNAs; as their names imply, importins mediate import while exportins mediate export (5-10). Common to these cofactors is the ability to bind RanGTP, the GTP-bound state of the small GTPase Ran. Recent research has suggested

---

This thesis follows the style and format of *The Journal of Biological Chemistry*.

that importins also function as chaperones by surrounding very basic regions of basic proteins, such as histones and ribosomal proteins, to prevent aggregation around polyanions in the cell (11). In some instances, an additional adapter importin, such as importin α, is necessary for importin β-mediated transport (5, 6).

The directionality of transport is controlled by the RanGTP gradient across the NE (5-9, 12). This gradient consists of a high RanGTP concentration in the nucleus and an abundance of RanGDP in the cytoplasm, yielding a nuclear to cytoplasmic RanGTP concentration ratio of ~500 (13). This RanGTP gradient is maintained by the chromatin-bound Ran guanine nucleotide exchange factor RCC1 (14), which efficiently catalyzes the loading of GTP (GDP/GTP exchange), and the cytoplasmic RanGTPase activating protein (RanGAP) and its accessory proteins RanBP1 and NPC-filament-bound RanBP2 (15, 16), which stimulate GTP hydrolysis (5-7, 9, 10). Importins bind their cargoes in the cytoplasm and binding of RanGTP to this importin-cargo complex in the nucleus results in a conformational change which releases the cargo (5-7, 9, 10, 17-19). In contrast, exportins must form a complex with RanGTP in the nucleus before they can recognize their intended cargoes. The entire exportin-RanGTP-cargo complex transits to the cytoplasm, where RanGAP-induced hydrolysis results in substrate release (5-7, 9, 10). Nuclear transport factor 2 (NTF2) is a transport receptor whose sole function is to facilitate the import of cytoplasmic RanGDP into the nucleus, where the GDP is quickly exchanged for GTP by RCC1 to maintain the RanGTP gradient (20-22).

As an example of the extensive traffic through NPCs, ribosome synthesis requires multiple NPC transport events. In order to build a ribosome, mRNA molecules are

exported from the nucleus to the cytoplasm, where they are translated into ~80 different ribosomal proteins. The ribosomal proteins are then imported into the nucleus where they are assembled with rRNA in the nucleoli to form ribosomal subunits. Importins recognize the nuclear localization signals (NLS) of various ribosomal proteins, assisting this import process (23). The large and small ribosomal subunits are exported to the cytoplasm where final assembly occurs, allowing them to catalyze mRNA translation into proteins.

We sought to characterize the import and export of cargoes through the NPC in live cells using fluorescently-tagged, recombinant human ribosomal protein L23a (rpL23a-His) as a model substrate. The rpL23a protein transits twice through the NPC, once as a freshly translated protein imported into the nucleus and once as part of the assembled large ribosomal subunit that is exported to the cytoplasm. Microinjection was employed to cytoplasmically introduce the rpL23a-His protein and epifluorescence microscopy was used to visualize the ribosomal proteins.

METHODS

Recombinant Ribosomal Protein L23a. The human ribosomal protein L23a (rpL23a) gene was amplified from IMAGE Clone 3140342 (ATCC MGC-15572) with the polymerase chain reaction (PCR) using the primers GCCCTCGAGCCGAAAGCGAAGAAGG and CCGGGATCCGATGATCCCAATTTTG and subcloned with XhoI and BamHI into the plasmid vector pTrcHisA (Invitrogen). This construct added a single cysteine followed by six histidines (6xHis) to the C-terminal end of rpL23a. The rpL23a gene, including the encoded 6xHis tag, was then PCR-amplified from this plasmid with primers CCGCCATGGAAAGACTCGAGCCGAAAGCG and GCCGTCGACCGCTACTGCCGCCAGGCAAATT and cloned into the pET28a vector (Novagen) with NcoI and SalI. This construct (encoding rpL23a-His) included a 3-base codon (GAA) for glutamic acid in the penultimate N-terminal position, conferring translational stability in *Escherichia coli*. This construct also places the rpL23a-His gene under the control of an isopropyl-β-D-thiogalactopyranoside- (IPTG) inducible T7 promoter for expression in *E. coli*. The coding region was confirmed by DNA sequencing to be rpL23a (NCB Accession #AAH58041) with the designed additions.

rpL23a-His Overexpression and Purification. The rpL23a-His plasmid construct described above was transformed into *E. coli* strain BL21 (λDE3) for overexpression. Cultures were grown with kanamycin (30 μg/mL) at 37 °C until an OD_{600} of ~1-2 and

induced with 1 mM IPTG for 4 hrs. Cell pellets were stored at -80 °C. For purification, cell pellets were thawed and resuspended in 50 mM Tris, 50 mM LiCl, 10 mM imidazole, pH 8.0 (resuspension buffer) at a ratio of 10 mL buffer to 1 g cells. After the addition of 4 mM β-mercaptoethanol (β-Me), 1 mM phenylmethylsulfonyl fluoride, 40 μg leupeptin, 0.4 mg soybean trypsin inhibitor, and 40 μg pepstatin A, resuspended cells were lysed by French Press (~3 times, ~15, 000 psi). The lysed cell solution was centrifuged (15, 000 g, 10 min) and one volume of 0.2 M CAPS, 10 mM imidazole, 2 M NaCl, 2 M urea, 1% polyvinylpyrrolidone (PVP; 40 kDa), pH 10.0 (2X binding buffer), equilibrated to 37 °C, was added to the supernatant. The solution was incubated at 37 °C for 1 hr to chemically decompose the RNA at the high pH. After RNA decomposition, the solution was centrifuged (10, 000 g, 10 min) and the supernatant was combined with 1 mL 50% Ni-NTA Superflow resin (Qiagen) equilibrated with 1X binding buffer for every 10 mL of solution. This resin solution was incubated at 4 °C with slow stirring for 1 hr. The resin was then loaded on a column and washed extensively, first with 100 mL 1X binding buffer and then with 50 mL 10 mM imidazole, 100 mM NaCl, pH 8.0. The rpL23a-His protein was eluted with 500 mM imidazole, 100 mM NaCl, pH 8.0. Elution fractions were combined and concentrated to a final volume of ~2 mL. The concentrated sample was further purified by Mono S (Amersham) cation exchange chromatography using 20 mM HEPES, pH 8.0 and a linear NaCl gradient. Pure rpL23a-His eluted at 1 M NaCl.

N-terminal Sequencing. In order to N-terminally sequence rpL23a-His (Protein Chemistry Laboratory, Texas A&M University), purified protein was electrophoresed on

a polyacrylamide gel and transferred to a polyvinylidene fluoride (PVDF) membrane via electro-blotting with 10 mM CAPS, 10% methanol, pH 11.0. The PVDF membrane was stained with 0.1% Ponceau S for 5 min and destained with water.

Labeling with Alexa555. Pure rpL23a-His was chemically labeled with the fluorescent dye Alexa555 maleimide (Molecular Probes). To ensure reduced cysteines, rpL23a-His was first incubated with a 10-fold molar excess of tris(2-carboxyethyl)phosphine hydrochloride for 10 min at room temperature. Next, a 20-fold molar excess of Alexa555 maleimide was added and the labeling reaction was allowed to proceed for 2 hrs at room temperature in the dark before being quenched with a 10-fold molar excess of β-Me. The dye-labeled protein was dialyzed against 1000 volumes of 50 mM HEPES, 50 mM NaCl, pH 7.5 for 2 days with three buffer changes to remove free dye. The Alexa555-labeled rpL23a-His was stored in 50 µL aliquots at -80 °C. Labeling efficiency was analyzed by comparison of labeled and unlabeled protein bands on a Coomassie-stained polyacrylamide gel.

Alexa555-labeled NLS-2xGFP. The model substrate, Alexa555-labeled NLS-2xGFP, was prepared as described (24).

Permeabilized HeLa Cell Nuclear Transport. HeLa cells (ATCC) were grown and permeabilized as described (24). Transport reactions with rpL23a-His (~0.1 µM) in 20 mM HEPES, 110 mM KOAc, 5 mM NaOAc, 2 mM MgOAc, 1 mM EGTA, 1.5% PVP

(360 kDa), pH 7.3 (transport buffer) included necessary transport cofactors (0.5 μM importin β, 2 μM Ran, 1 μM NTF2, and 1 mM GTP) isolated as described (24). After 10 min transport reactions, cells were washed with transport buffer. Transport reactions using NLS-2xGFP were performed as detailed (24).

Microinjection. Freshly split HeLa cells were grown overnight at 37 °C with 5% CO_2 in Dulbecco's Modified Eagle Medium (D-MEM; GIBCO) supplemented with 4.5 g/L glucose, 862 mg/L GlutaMAX-I, and phenol red indicator, 100 U/mL penicillin, 100 μg/mL streptomycin, and newborn calf serum in glass-bottom petri dishes (MatTek Corporation). Immediately prior to microinjections, the media was replaced with an identically supplemented D-MEM without phenol red. Microinjection was carried out with an Eppendorf FemtoJet utilizing needles with 0.5 μm ± 0.2 μm diameter tips (Original Eppendorf Femtotips) and loaded with transport substrates diluted to ~1 μM with 10 mM Tris, 100 mM NaCl, 0.1% PVP (40 kDa).

Epifluorescence Microscopy. Fluorescent rpL23a-His was visualized in permeabilized and microinjected HeLa cells with a Zeiss Axiovert 200M inverted microscope equipped with a Zeiss 1.45 NA 100X oil immersion objective, a CoolSnap ES high-resolution CCD camera (Roper Scientific), and a Prior ProScan II motorized stage. For microinjections, the objective was warmed with a Bioptechs objective heater to 37 °C; the immersion oil mediated heat transfer to the sample coverslip and maintained sample temperature at 37 °C. MetaMorph (Universal Imaging) software was used to control the microscope and

collect and analyze data. Differential interference contrast (DIC) microscopy was used for cell visualization during microinjections. All images were captured with 91 ms integration.

RESULTS

Project Design. The goal of this research was to investigate the nuclear transport and trafficking properties of ribosomal proteins and assembled ribosomal subunits through NPCs in living, mammalian cells. In order to directly observe these events, a sensitive method was required to detect these proteinaceous macromolecules in live cells. The strategy utilized was to fluorescently tag a purified, human ribosomal protein and introduce it into intact HeLa cells. The expectation was that once presented into the cytoplasmic region of the cell, the dye-labeled protein could be tracked as it migrated from the cytosol to the nucleus through the NPC, transited to the nucleolus for integration in ribosomal subunits, and finally re-transported through the NPC back into the cytoplasm as a part of an assembled ribosomal subunit.

Given that a eukaryotic ribosomal structure has not yet been obtained, the three-dimensional crystal structure of the large ribosomal subunit from the bacterium *Haloarcula marismortui* (PDB #1FFK) was used to select an appropriate ribosomal protein for dye labeling. Ribosomal protein L23a was selected for three reasons: 1) the protein is peripherally bound to the assembled large ribosomal subunit and thus dye attachment was not anticipated to influence function or assembly; 2) it contains no cysteine residues so a cysteine can be judiciously introduced for specific chemical attachment of the dye; and 3) the C-terminus is solvent exposed such that the addition of a C-terminal 6xHis-tag was not expected to alter structure or function. Having chosen the ribosomal protein, we proceeded to add a C-terminal tag consisting of a single

cysteine, for labeling with a single dye molecule, and six consecutive histidine residues, for purification purposes.

Cloning, Overexpression, Purification, and Dye Labeling. The DNA and protein sequences for rpL23a-His are shown in Figure 1. The plasmid demonstrated excellent overexpression of the rpL23a-His protein upon IPTG induction (Figure 2a). While the expected molecular weight (MW) of rpL23a-His is ~19 kDa, the protein migrates at a larger apparent MW on denaturing polyacrylamide electrophoresis gels (~24 kDa) due to its highly basic nature (25). The rpL23a-His protein was purified from cell lysates by means of Ni-NTA metal chelate affinity chromatography. Urea (1 M) dramatically improved 6xHis-tag binding to Ni-NTA, presumably by slightly denaturing the protein and thereby unmasking an obscured C-terminus. Minimal binding of rpL23a-His to charged Ni-NTA resin occurred in the absence of urea (not shown). Analysis of the Ni-NTA eluates revealed the presence of two major proteins (Figure 2b). These fractions were pooled and further purified with cation exchange chromatography, resulting in a single fraction of pure rpL23a-His which eluted at 1 M NaCl on a linear NaCl gradient. The remaining samples still contained two protein products (Figure 3); N-terminal sequences of these proteins are identified in Figure 1. Considering that its Ni-NTA purification confirmed presence of the C-terminal 6xHis-tag and that sequencing revealed the correct N-terminus, the higher-MW band was determined to be full-length rpL23a-His. The lower-MW band was two truncated products; one was shortened after the 24^{th} residue while the other was curtailed after the 26^{th} amino acid. Re-purification

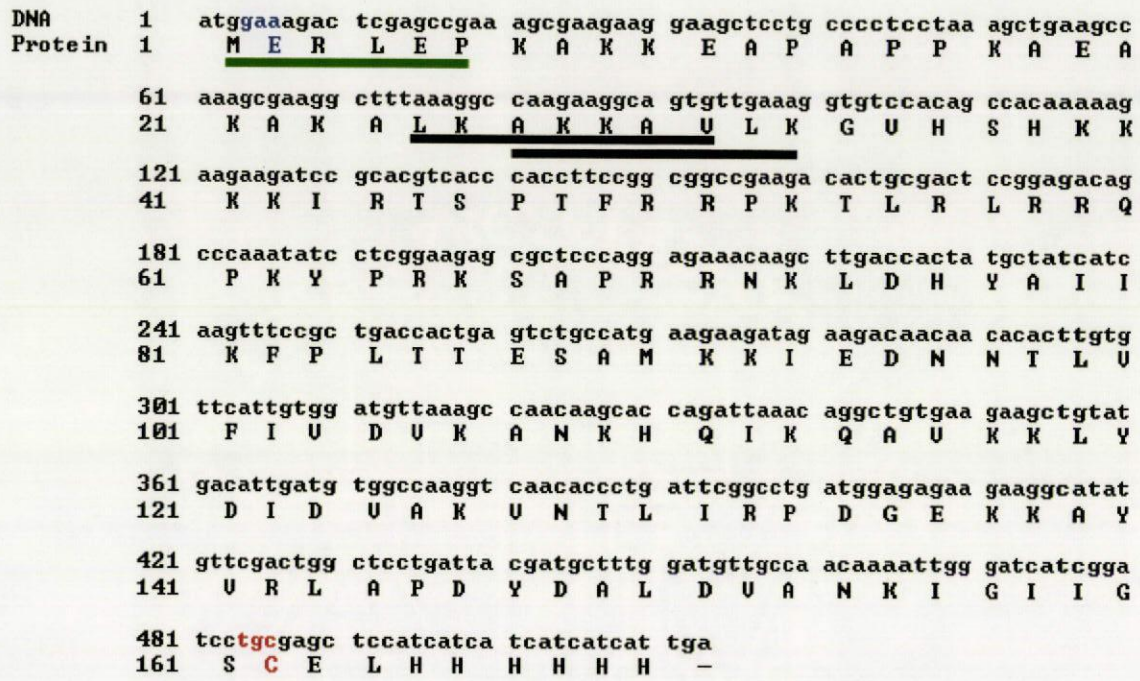

Figure 1. DNA sequence and primary structure for rpL23a-His. The glutamic acid residue (E; blue), provides translational stability. The single cysteine (C; red) was introduced to allow labeling by Alexa555 maleimide. The recombinant protein ends in six C-terminal histidines. Amino acid sequences identified for proteins from SDS-PAGE gels by N-terminal sequencing are underlined in green (full-length protein) and black (truncated proteins).

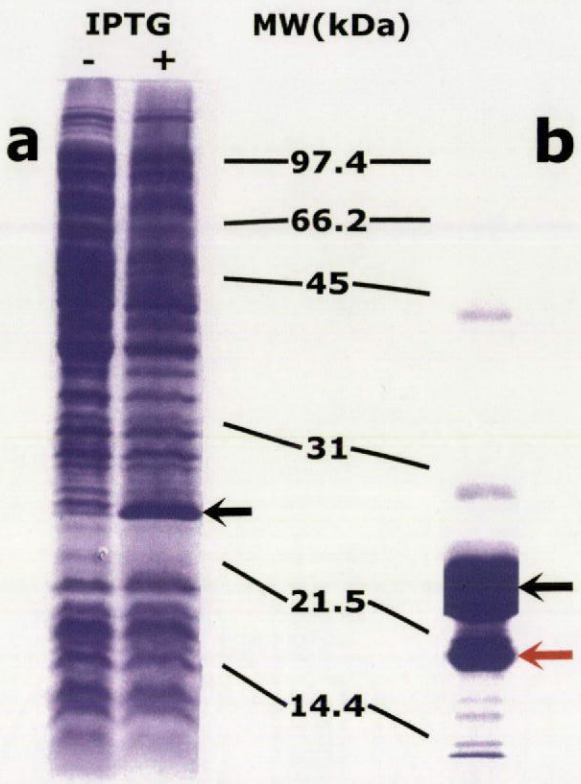

Figure 2. *E. coli* overexpression and Ni-NTA purification of rpL23a-His. **(a)** Coomassie-stained SDS-PAGE gel of cells with (+) and without (-) IPTG induction. The rpL23a-His protein (black arrow) is easily identified in the induced cells by the dark band at ~24 kDa, as indicated. **(b)** SDS-PAGE gel with Coomassie blue staining of elution from rpL23a-His purification by Ni-NTA metal chelate affinity chromatography. N-terminal sequencing revealed that the heavier band (black arrow) is full-length rpL23a-His (green line, Figure 1) and the lighter band (red arrow) represents two truncated products (black lines, Figure 1).

Figure 3. Purification of NiNTA-purified rpL23a-His by Mono S cation exchange chromatography. Chromatogram of Mono S purification. Absorbance (280 nm), blue; fractions, red; percent 2 M NaCl, green. **(inset)** Analysis of elution fractions 37-58 and 65-66 with SDS-PAGE and Coomassie blue staining. The rpL23a-His protein eluted as the major band, but truncated rpL23a-His proteins were observed in all fractions but fraction 37, which was pure rpL23a. The eluate fractions were not otherwise contaminated, suggesting full-length rpL23a-His was purified, but interaction with the Mono S column caused truncation.

Absorbance (mAU)
0
200
400
600
Elution Fractions
MW(kDa)
97.4
66.2
45
31
21.5
37 38 39 40 41 42 43 44 45 46 47 48 49 50 51 52 53 54 55 56 57 58 65 66
rpl23a-His
truncated rpL23a-His
% 2 M NaCl
0
20
40
60
80
100
Volume (mL)
0.0
10.0
20.0
30.0

of pure rpL23a-His through the same cation exchanger revealed an identical pattern of protein elution, indicating protein cleavage on the column. The pure rpL23a-His produced a single band on a Coomassie-stained SDS-PAGE gel even after extensive storage at -20 °C (>15 days) (not shown), confirming that the decomposition was not self-catalytic.

The pure rpL23a-His was chemically labeled with Alexa555 maleimide. A 20-fold excess of dye resulted in only a 41% labeling efficiency (Figure 4). A buried C-terminus could be the cause of the low labeling efficiency, as the C-terminal 6xHis-tag does not bind well to Ni-NTA resin in the absence of 1 M urea (see above).

Nuclear Import in Permeabilized Cells. With a pure, Alexa555-labeled protein in hand, the next step was to verify that the protein behaved as expected in permeabilized HeLa cell transport reactions. Transport reactions performed with an excess of transport cofactors (Methods) in permeabilized HeLa cells showed a nuclear accumulation of rpL23a-His with concentration in the nucleolus (Figure 5). This distribution differs from the nearly homogeneous nuclear localization of NLS-2xGFP, a foreign protein carrying a nuclear localization signal, in permeabilized cells (Figure 6). The addition of importin α (0.5 μM) to the other cofactors, necessary for NLS-2xGFP import, actually hindered the import of rpL23a-His, while the exclusion of all transport cofactors resulted in an absence of transport (not shown). These observations agree with previously published results of rpL23a import in permeabilized HeLa cells (23) and indicate that rpL23a import is importin β-dependent. The results of the permeabilized transport reaction indicate

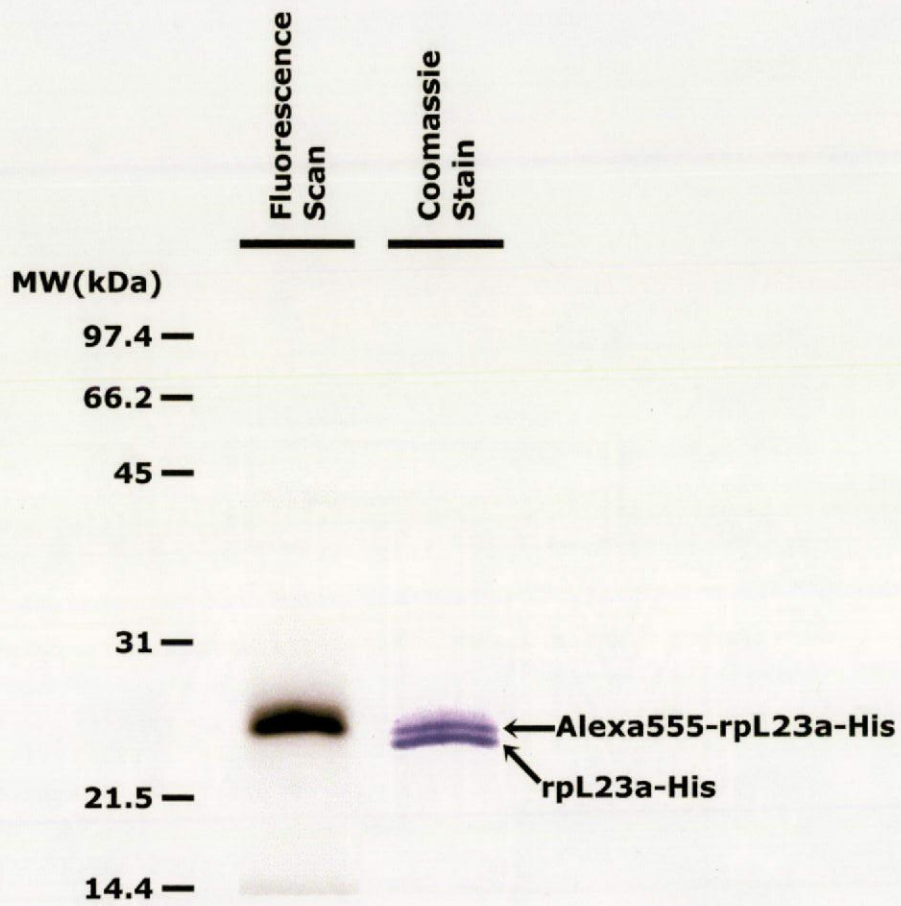

Figure 4. Alexa555 labeling of rpL23a-His. Pure rpL23a-His was labeled with Alexa555 maleimide (Methods) and the electrophoresed product was analyzed by Coomassie staining and fluorescence scanning (Ex = 546 nm). Of the two bands observed by Coomassie stain, only the upper one was fluorescent. Intensity comparison revealed a labeling efficiency of 41%.

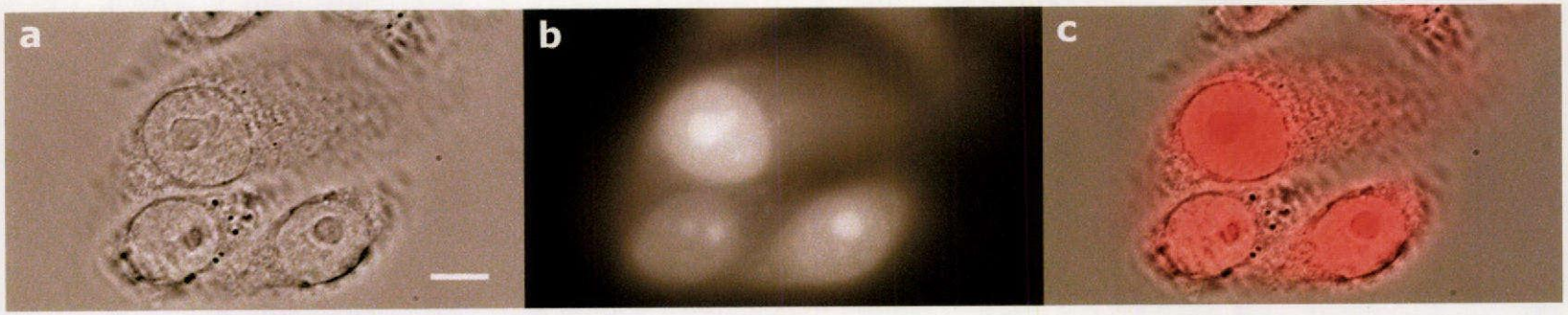

Figure 5. Nuclear import and nucleolar localization of rpL23a-His in permeabilized HeLa cells. Alexa555-labeled rpL23a-His was transported into the nuclei of permeabilized HeLa cells (Methods). **(a)** DIC image. **(b)** Alexa555 Fluorescence. **(c)** Merged image with the signal in (b) shown in red. 100X magnification. Scale bar: 10 μm.

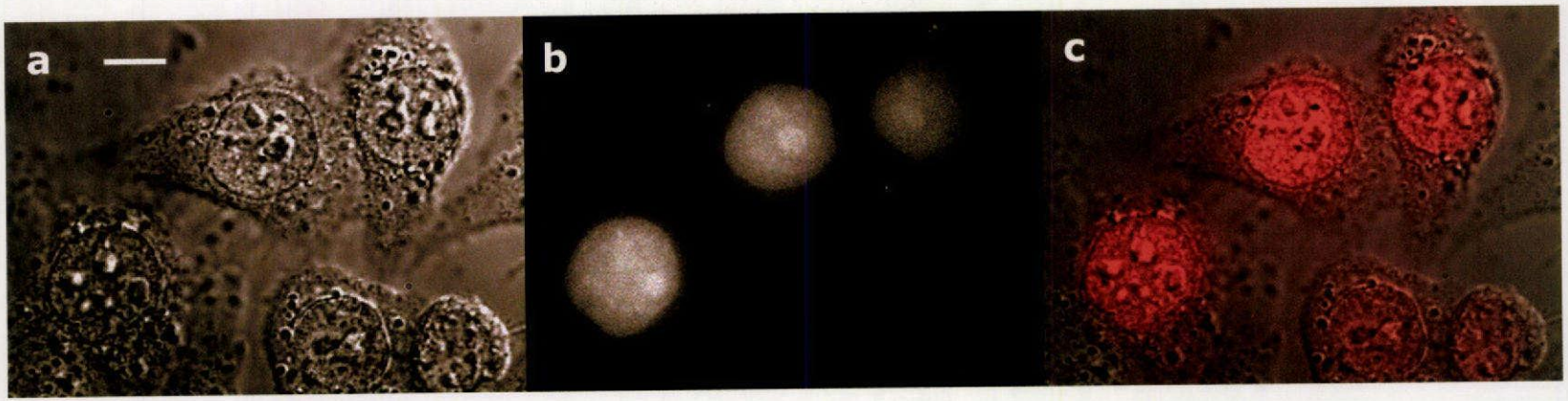

Figure 6. Nuclear import of NLS-2xGFP in permeabilized HeLa cells. Alexa555-labeled rpL23a was transported into the nuclei of permeabilized HeLa cells (Methods). **(a)** DIC image. **(b)** Alexa555 fluorescence. **(c)** Merged image with the signal in (b) shown in red. 100X magnification. Scale bar: 10μm.

proper targeting of rpL23a-His to the nucleus and to the nucleolus.

Nuclear Import in Live Cells. With pure, labeled rpL23a-His exhibiting expected behaviors and properties in permeabilized cells, it was introduced into living HeLa cells. Alexa555 fluorescence in microinjected cells was monitored over time and images were assembled to display the fluorescence pattern at various stages after injection (Figure 7). Immediately after injection, the protein promptly accumulated in the nucleus. Soon afterwards, the fluorescent proteins gradually exited the nucleus, evidenced by the diminishing nuclear intensity over time. The intensity of the cytoplasm remained nearly constant, arguing against photobleaching as the cause of the decreasing nuclear intensity. As rpL23a-His departed the nucleus, it collected in various regions of the cytoplasm forming bright, mobile spots. The nucleoli remained minimally inhabited for the duration of the observation.

As a control experiment, we tested the ability of intact HeLa cells to import the model substrate NLS-2xGFP, which contains both a 6xHis-tag and Alexa555 dyes. This substrate contains a nuclear localization signal (NLS) which targets it for importin α/β-dependent transport (5, 6). Because the NLS-2xGFP protein serves no purpose in HeLa cells and is not equipped with a nuclear export signal, the injected protein was expected to remain in the nucleus after import. This was, in fact, exactly what was observed (Figure 8). Further, the nucleoli of the injected cells remained dim; since the nucleoli are the sites of ribosomal subunit assembly and NLS-2xGFP plays no role in this process, it is not surprising that NLS-2xGFP was excluded from nucleoli. This exclusion is not

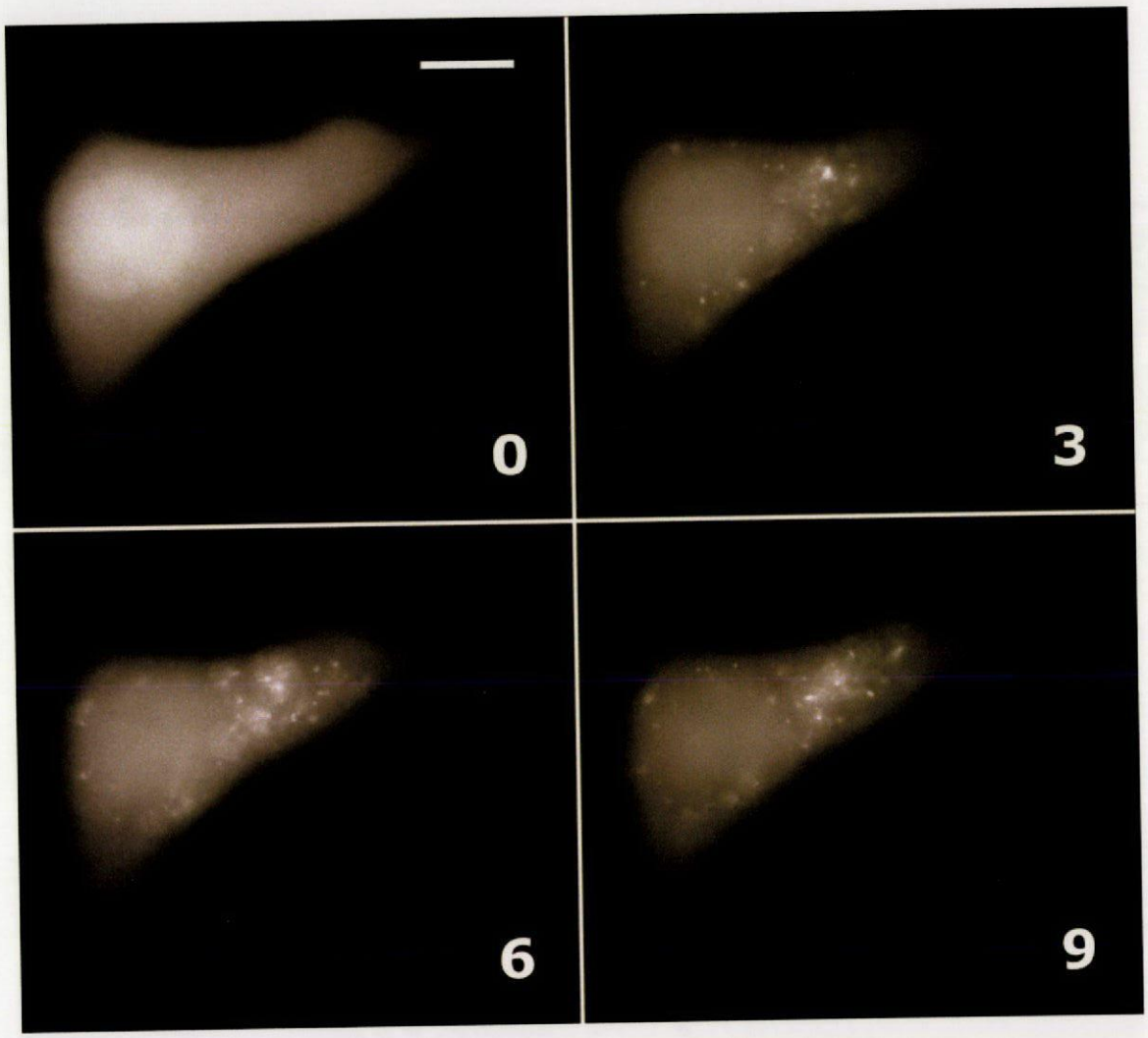

Figure 7. Time-lapse images of rpL23a-His microinjected into intact HeLa cells. Fluorescence observed in a single HeLa cell cytoplasmically microinjected with rpL23a-His (Methods). Numbers show time (minutes) after injection. 100X magnification, 37 °C. Scale bar: 10 μm.

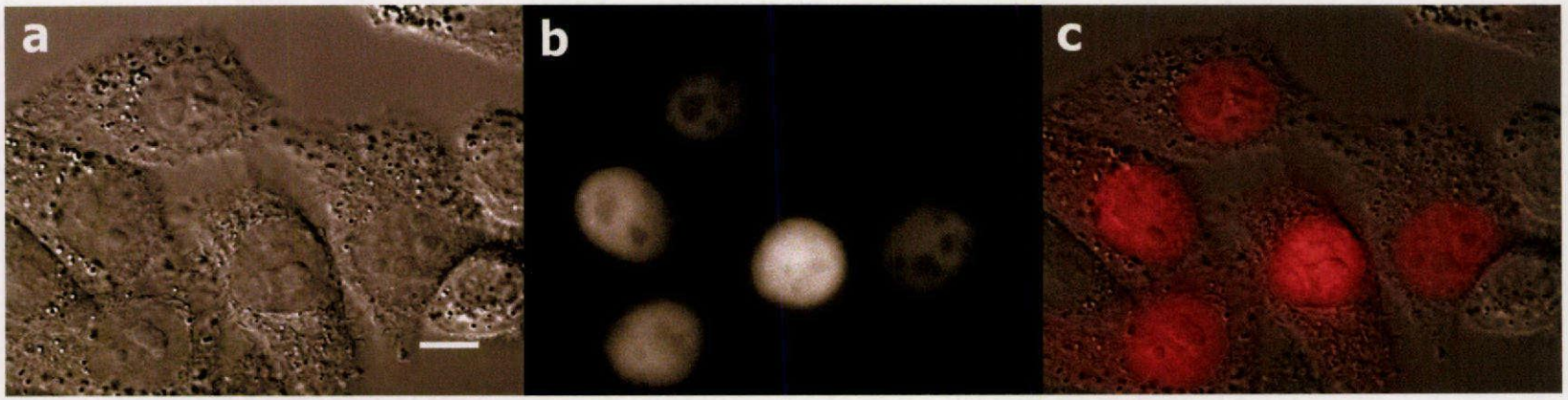

Figure 8. Microinjection of the model substrate, Alexa555-labeled NLS-2xGFP. Intact HeLa cells were cytoplasmically microinjected with Alexa555-labeled NLS-2xGFP and fluorescence was observed ~5 sec after injection (Methods). **(a)** DIC image. **(b)** Alexa555 fluorescence. **(c)** Merged image with the signal in (b) shown in red. 100X magnification, 37 °C. Scale bar: 10 μm.

observed in permeabilized cells because permeabilization kills the cells, therefore halting the manufacture of ribosomal subunits. The success of this control experiment implies that the presence of Alexa555 dye molecules and a 6xHis-tag do not adversely affect the cell, nor do they hinder the proper nuclear import of the target protein. The ability of the NLS-2xGFP protein to transport across the NE also indicates sufficient transport cofactors in the living cells for the concentration of transport substrate injected.

DISCUSSION AND CONCLUSIONS

Cytoplasmic ribosomes synthesize eukaryotic ribosomal proteins, which transit into the nucleus through NPCs for assembly into ribosomal subunits in the nucleoli. Upon completion, the large and small ribosomal subunits must traffic to the NE and transit through NPCs to the cytoplasm, where they fulfill their physiological niche of catalyzing and controlling protein synthesis. Therefore, by fluorescently tagging a single ribosomal protein, the expectation was that this protein, rpL23a-His, would be observed transiting into the nuclei, and nucleoli, of live cells; then, after some delay, which reports the time-scale of assembly into the large ribosomal subunit, the fluorescent protein would leave the nucleus as part of an assembled ribosomal subunit. The observed behavior, however, was somewhat different. Immediately after microinjection, rpL23a-His rapidly accumulated in the nucleus, indicating very efficient import of cytoplasmic rpL23a. After the initial nuclear influx, however, rpL23a-His was gradually exported, as indicated by a steadily decreasing nuclear intensity of Alexa555 dye, and localized at various, discrete locations within the cytoplasm, as indicated by bright, mobile spots. Most surprising was the strong lack of nucleolar localization in the microinjected cells.

There are multiple explanations for the observation that nucleoli remain weakly inhabited with rpL23a-His throughout the observation time. The overall assembly of the ribosomal subunit could be incredibly fast, or the incorporation of rpL23a could be one of the final steps of the process, limiting the amount of time rpL23a spends at the nucleoli before the ribosomal subunits transit to the cytoplasm. Alternatively, the lack of nucleolar localization could be caused by unfavorable conditions imposed upon the cell

by microinjection of a large amount of rpL23a-His; for instance, by overloading the capacity of the nucleoli to make ribosomes.

The bright, fluorescent spots within the cytoplasm after nuclear export of Alexa555 fluorescence are not believed to represent functional, assembled ribsomes. Free ribosomes are distributed throughout the cytoplasm of the cell while membrane-bound ribosomes are attached to the rough endoplasmic reticulum (ER). Thus, exported rpL23a-His should yield fluorescence homogeneously distributed within the cytoplasm and possibly outlining the rough ER as a consequence of the congregation of ribosomes. The well-separated bright spots observed, therefore, do not appear to be functioning ribosomes. These spots are scattered throughout the cytoplasm and appear to move randomly, whereas ER-bound ribosomes would be fairly immobile. Perhaps too much rpL23a-His was introduced into the HeLa cell and the bright spots resulted from an effort by the cell to combat the excess protein. In this vein, it is conceivable that the bright spots represent lysosomal compartments to which the excess ribosomal protein was targeted for degradation. Another possible cause of the bright spots is the aggregation of rpL23a-His on polyanions such as RNA. It is believed that some members of the importin transport cofactor family, specifically importins 5 and 7 for rpL23a, function as chaperones for highly basic proteins, binding to their basic regions and thus preventing their aggregation on polyanions (11). It was shown that physiological levels of these importins is sufficient to prevent aggregation (11), but perhaps the flood of rpL23a-His from microinjection overwhelmed the cell's protective capacity.

We have taken many steps forward towards characterizing the *in vivo* properties of NPCs. We have successfully isolated and fluorescently-tagged a recombinant human ribosomal protein. We demonstrated that this fluorescent substrate is properly targeted and localized in permeabilized cells based on published results and control studies. These targeting studies led us to cytoplasmic microinjection of rpL23-His into intact HeLa cells, where we confirmed that the ribosomal protein first transits into the nucleus and is later exported. In future studies, we will analyze the minimally inhabited nucleoli and bright spots observed in these microinjections by attempting injections with a much diluted rpL23a-His. If these observations resulted from an excess of rpL23a-His, the diluted injections would eliminate such phenomena. Ultimately, we plan on observing the behavior of single rpL23a-His molecules as they transit into the nucleus, integrate into a ribosomal subunit in the nucleoli, and export into the cytoplasm as part of an assembled large ribosomal subunit. Recently, our lab visualized and kinetically characterized single transport events across the NE of permeabilized cells, suggesting that similar observations are feasible in live cells (24). This will allow characterization of the *in vivo* kinetics of NPC transport and the order and kinetics of ribosomal protein addition to assembling ribosomal subunits.

REFERENCES

1. Paine, P. L., Moore, L. C., and Horowitz, S. B. (1975) *Nature* **254,** 109-114
2. Pante, N., and Kann, M. (2002) *Mol. Biol. Cell* **13,** 425-434
3. Breeuwer, M., and Goldfarb, D. S. (1990) *Cell* **60,** 999-1008
4. Pruschy, M., Ju, Y., Spitz, L., Carafoli, E., and Goldfarb, D. S. (1994) *J. Cell Biol.* **127,** 1527-1536
5. Mattaj, I. W., and Englmeier, L. (1998) *Annu. Rev. Biochem.* **67,** 265-306
6. Görlich, D., and Kutay, U. (1999) *Annu. Rev. Cell Dev. Biol.* **15,** 607-660
7. Macara, I. G. (2001) *Microbiol. Mol. Biol. Rev.* **65,** 570-594
8. Lei, E. P., and Silver, P. A. (2002) *Dev. Cell* **2,** 261-272
9. Weis, K. (2002) *Curr. Opin. Cell Biol.* **14,** 328-335
10. Weis, K. (2003) *Cell* **112,** 441-451
11. Jäkel, S., Mingot, J. M., Schwarzmaier, P., Hartmann, E., and Görlich, D. (2002) *EMBO J.* **21,** 377-386
12. Görlich, D., Pante, N., Kutay, U., Aebi, U., and Bischoff, F. R. (1996) *EMBO J.* **15,** 5584-5594
13. Smith, A. E., Slepchenko, B. M., Schaff, J. C., Loew, L. M., and Macara, I. G. (2002) *Science* **295,** 488-491
14. Ohtsubo, M., Okazaki, H., and Nishimoto, T. (1989) *J. Cell Biol.* **109,** 1389-1397

15. Yokoyama, N., Hayashi, N., Seki, T., Pante, N., Ohba, T., Nishii, K., Kuma, K., Hayashida, T., Miyata, T., Aebi, U., Fukui, M., and Nishimoto, T. (1995) *Nature* **376,** 184-188

16. Wu, J., Matunis, M. J., Kraemer, D., Blobel, G., and Coutavas, E. (1995) *J. Biol. Chem.* **270,** 14209-14213

17. Vetter, I. R., Arndt, A., Kutay, U., Görlich, D., and Wittinghofer, A. (1999) *Cell* **97,** 635-646

18. Cingolani, G., Petosa, D., Weis, K., and Muller, C. W. (1999) *Nature* **399,** 221-229

19. Bayliss, R., Littlewood, T., and Stewart, M. (2000) *Cell* **102,** 99-108

20. Ribbeck, K., Lipowsky, G., Kent, H. M., Stewart, M., and Görlich, D. (1998) *EMBO J.* **17,** 6587-6598

21. Smith, A., Brownawell, A., and Macara, I. G. (1998) *Curr. Biol.* **8,** 1403-1406

22. Ribbeck, K., and Görlich, D. (2001) *EMBO J.* **20,** 1320-1330

23. Jäkel, S., and Görlich, D. (1998) *EMBO J.* **17,** 4491-4502

24. Yang, W., Gelles, J., and Musser, S. M. (2004) Submitted to *Nature* (Tracking number: 2004-04-17951)

25. Hames, B. D. (1998) *Gel Electrophoresis of Proteins: A Practical Approach,* 3rd Ed., pp. 13-33, Oxford University Press, Oxford

VITA

Jason Wang
1919 Palencia Court
Arlington, Texas 76006
jasonwang@neo.tamu.edu
(817) 680-1178

Education

Bachelor of Science in Genetics and Biochemistry — August 2000 - May 2004
Texas A&M University, College Station, Texas

Research

University Undergraduate Research Fellow — August – May 2004
Texas A&M University, Lab of Dr. Siegfried Musser
"Real-Time Trafficking and Assembly of Ribosomal Subunits"

Distinguished Biochemistry Research Scholar — August – May 2004
Texas A&M University, Lab of Dr. Siegfried Musser
"Real-Time Trafficking and Assembly of Ribosomal Subunits"

Lecture: "Real-Time Trafficking and Assembly of Ribosomal Subunits" — March 2004
Student Research Week, Texas A&M University

Poster: "Real-Time Trafficking and Assembly of Ribosomal Subunits" — July 2002
Summer Undergraduate Research Program, Texas A&M Health Science Center

Summer Undergraduate Research Fellow — May – July 2002
Texas A&M Health Science Center, Lab of Dr. Siegfried Musser
"Real-Time Trafficking and Assembly of Ribosomal Subunits"

Honors, Awards, and Associations

University Honors — May 2004
Foundation Honors — May 2004

Academic Incentive Award — August – May 2004
Van Edwards Scroggins Memorial Scholarship — August – May 2004
Herman F. Heep Scholarship for Academic Excellence — August – May 2004

Sigma Xi, The Scientific Research Society; Associate Member — March 2004 – Present
Phi Kappa Phi Honor Society — May 2003 – Present
Golden Key International Honor Society — January 2002 – Present
National Society of Collegiate Scholars — January 2001 – Present
Phi Eta Sigma Honor Society — January 2001– Present